

THE JOURNAL OF PHYSICAL CHEMISTRY A

Supporting Information

Application of Time Dependent Density Functional and Natural Bond Orbital Theories to the UV/Vis Absorption Spectra of Some Phenolic Compounds

Svetlana Marković^{*} and Jelena Tošović

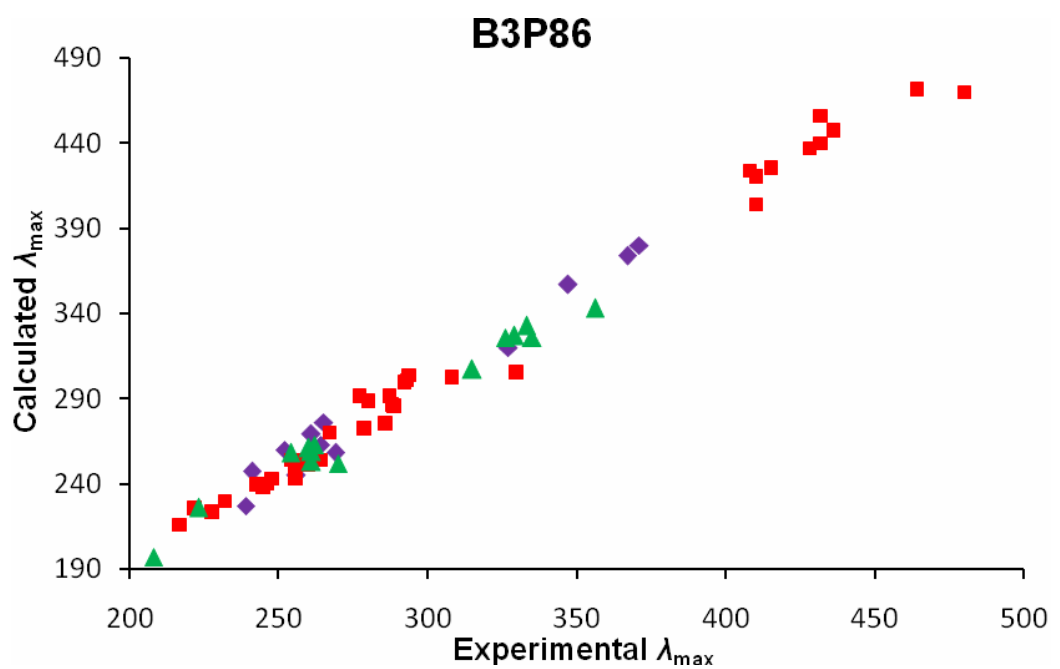
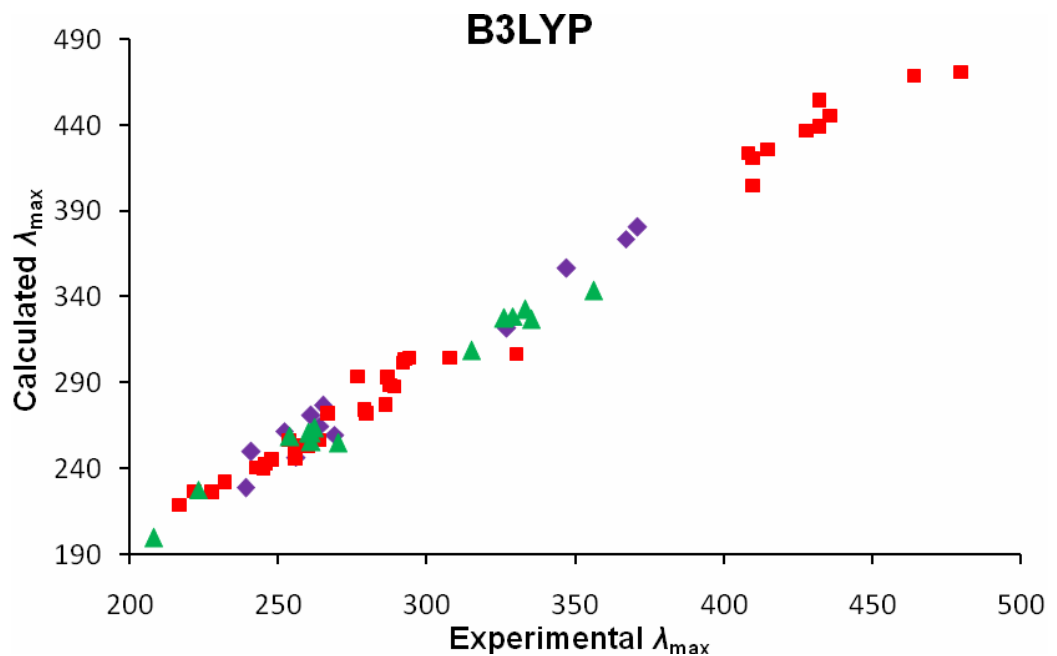
Department of Chemistry, Faculty of Science, University of Kragujevac

12 Radoja Domanovića, 34000 Kragujevac, Serbia

Corresponding author's e-mail address: mark@kg.ac.rs

Corresponding author's postal address: Faculty of Science, University of Kragujevac P.O. Box 60, 34000 Kragujevac, Serbia

Corresponding author's telephone and fax numbers: +381 34 335039, +381 34 335040



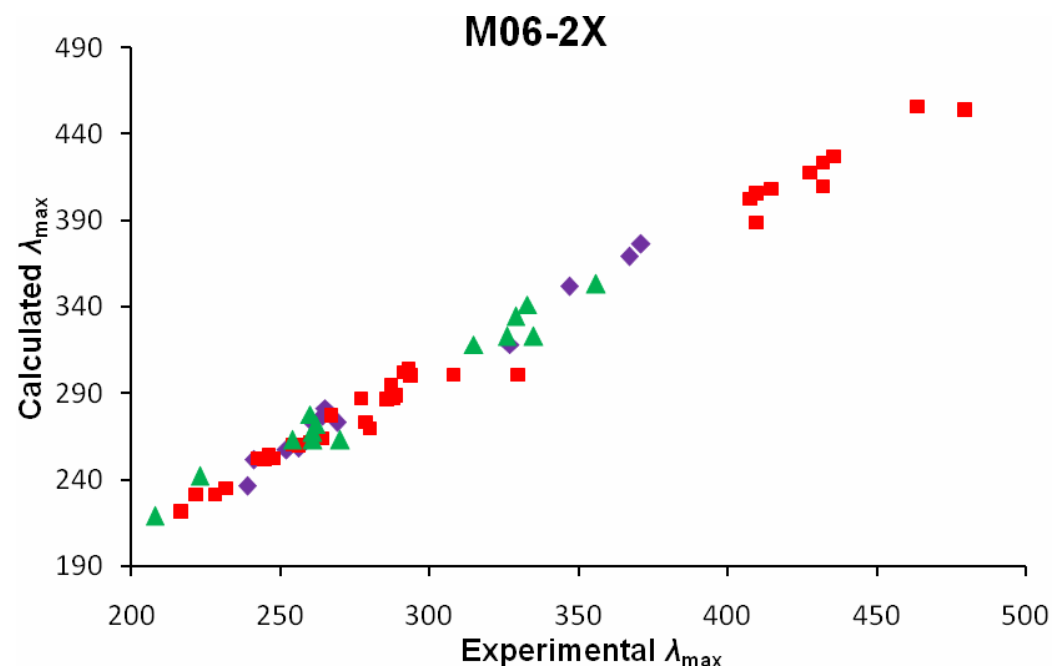
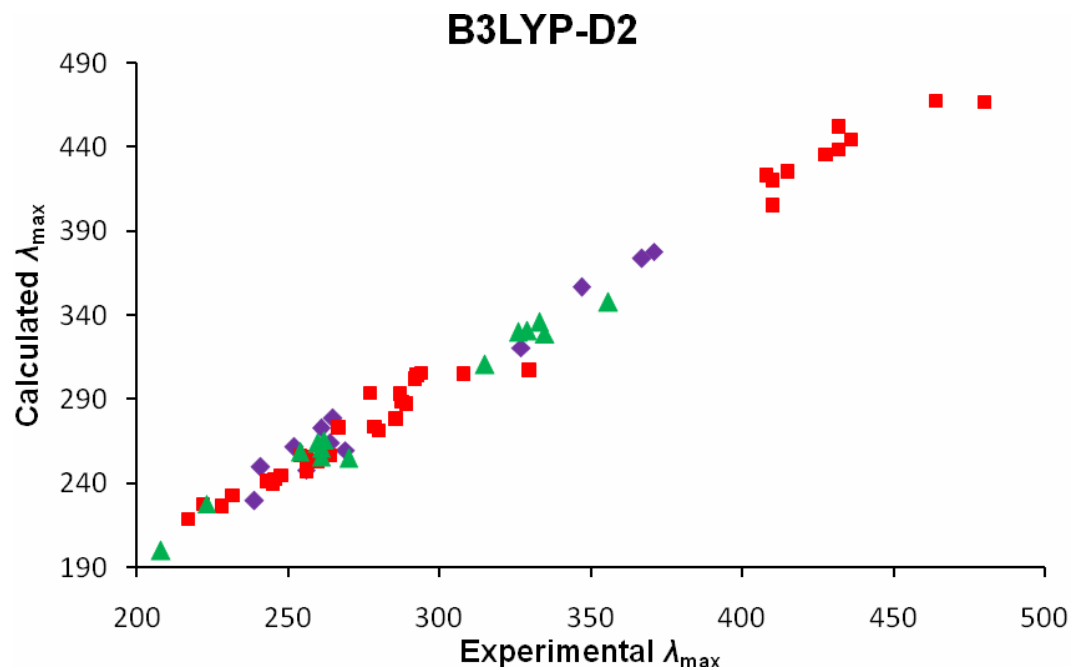


Figure S1. Correlation between the calculated and experimental λ_{\max} values for the applied methods. Red squares, green triangles, and purple rhombuses denote anthraquinones, neoflavonoids, and flavonoids, respectively. The scaled values from M06-2X are presented.

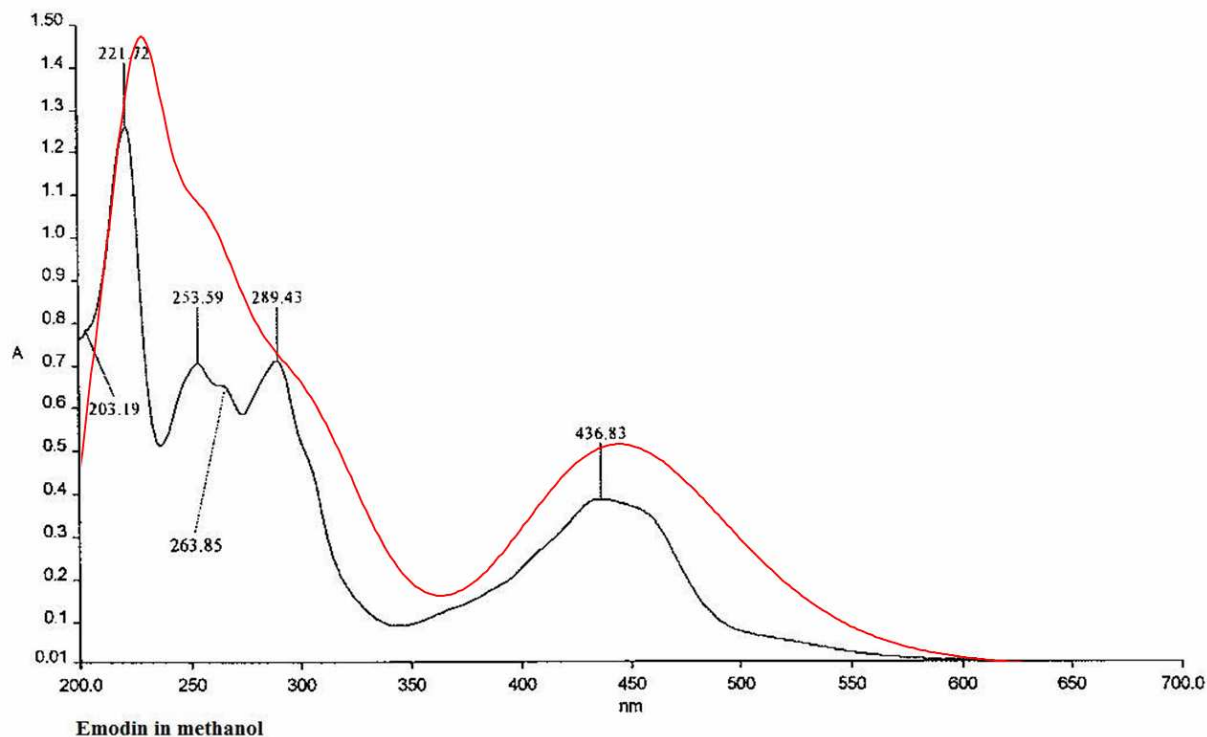


Figure S2. Experimental (black) and simulated (red) UV/Vis spectra for emodin.

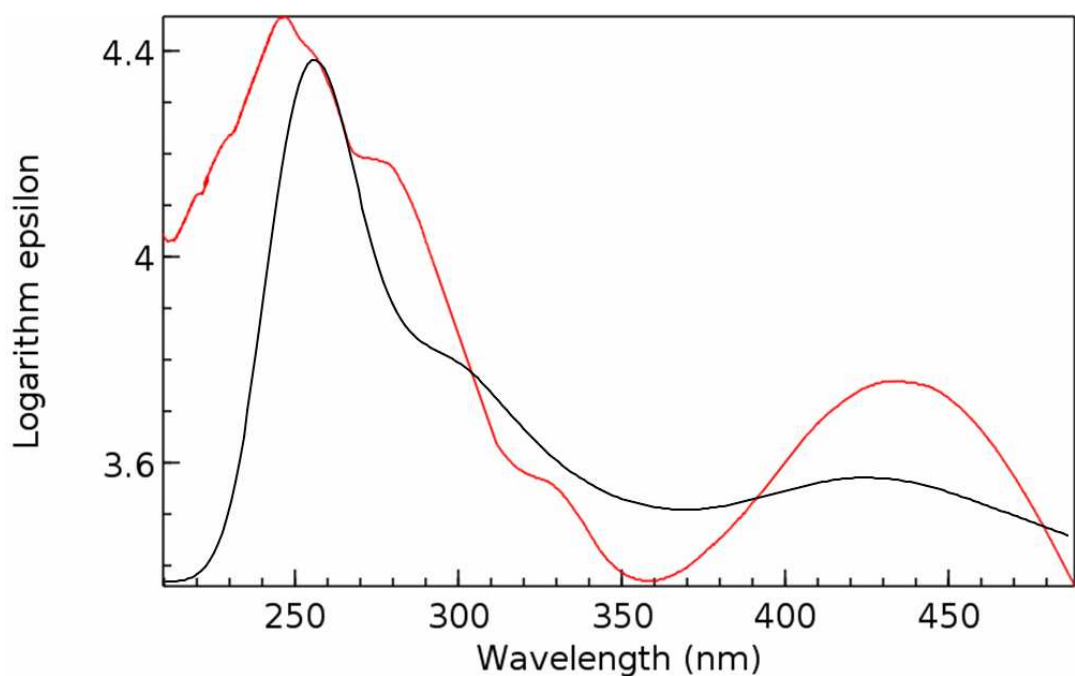


Figure S3. Experimental (red) and simulated (black) UV/Vis spectra for alizarin.

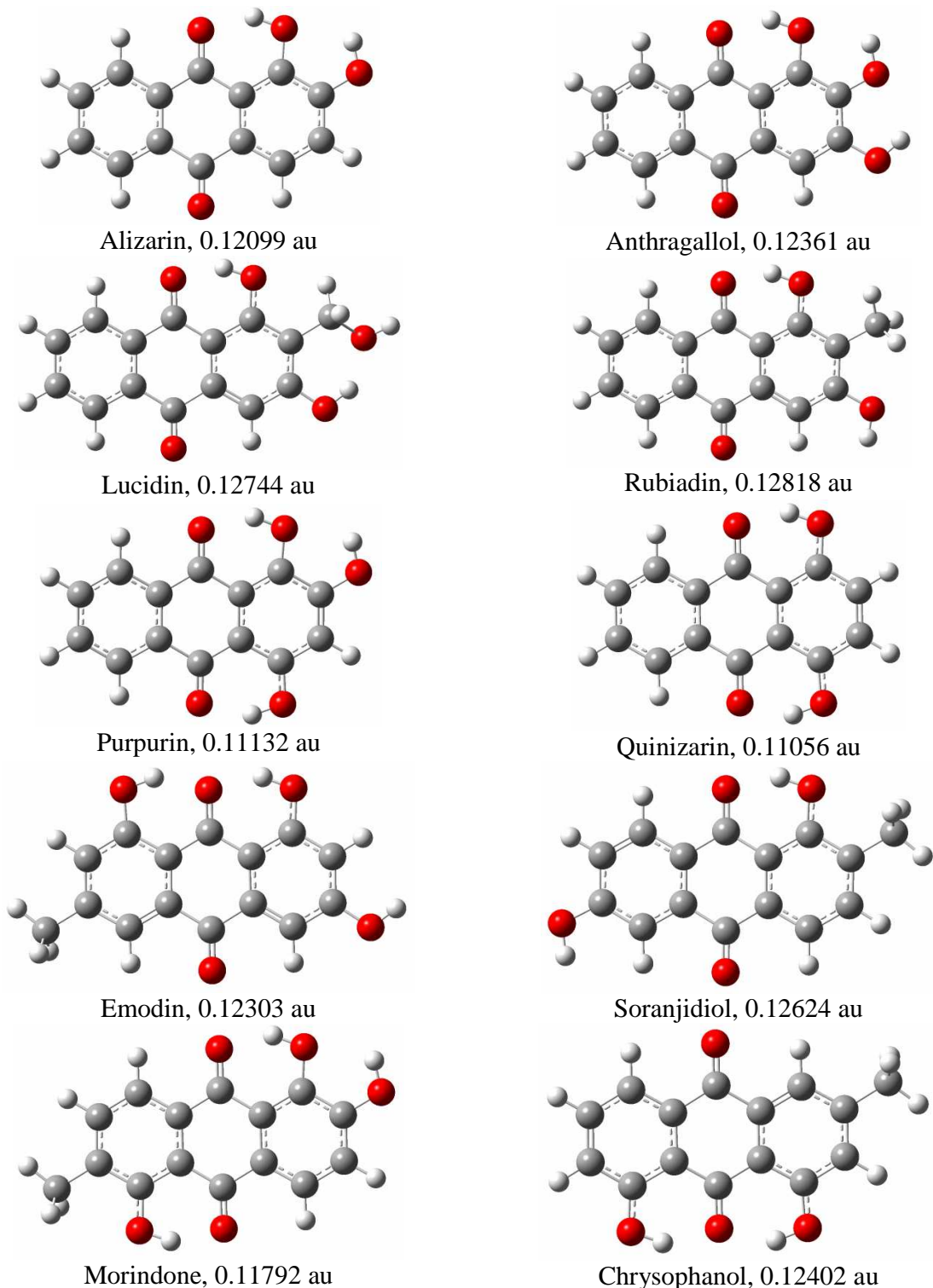


Figure S4. Geometries of the investigated phenolic anthraquinones optimized with the B3LYP functional, with the HOMO-LUMO gap values ($E_h/\text{particle}$) indicated.

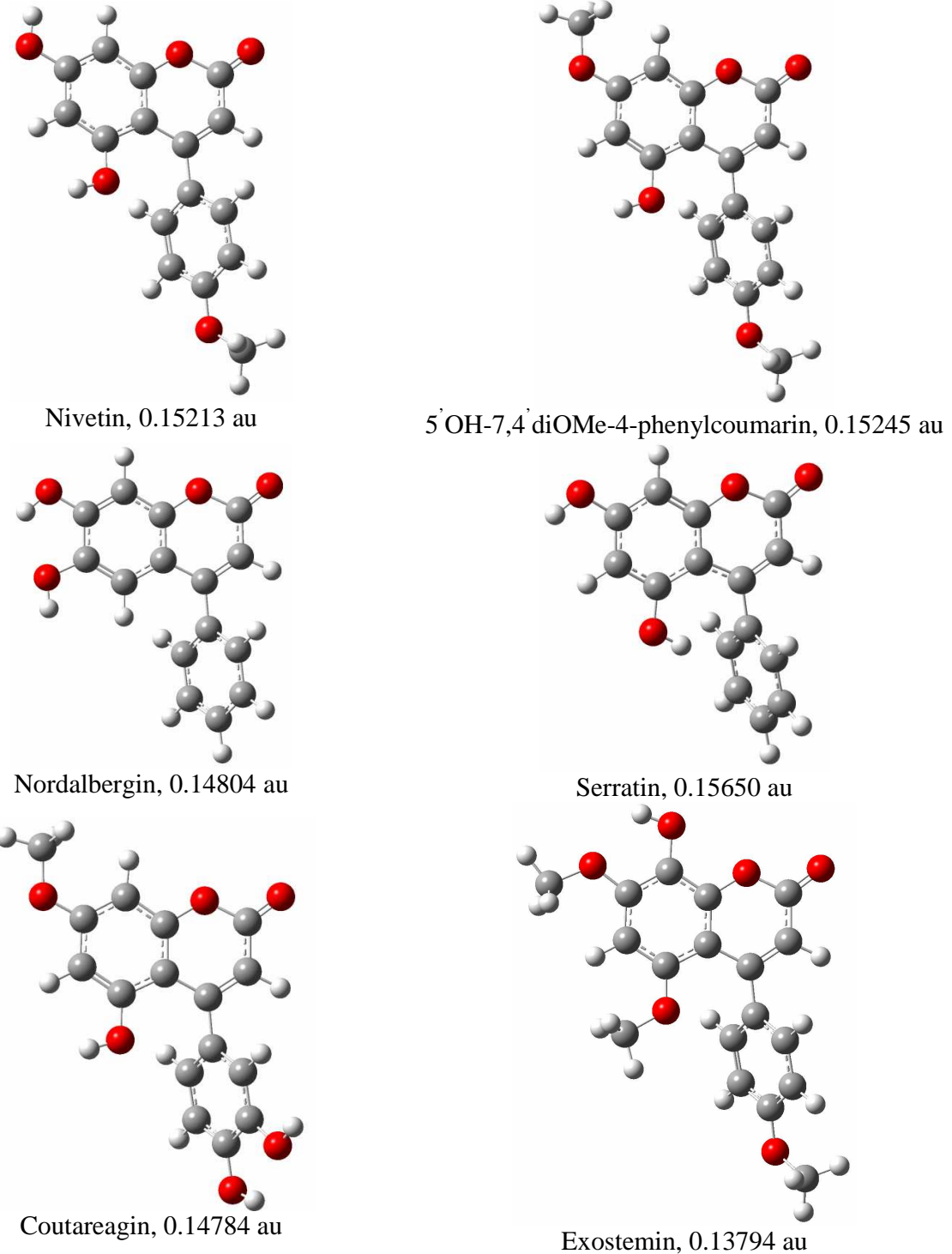


Figure S5. Geometries of the investigated neoflavonoids optimized with the B3LYP functional, with the HOMO-LUMO gap values ($E_h/\text{particle}$) indicated.

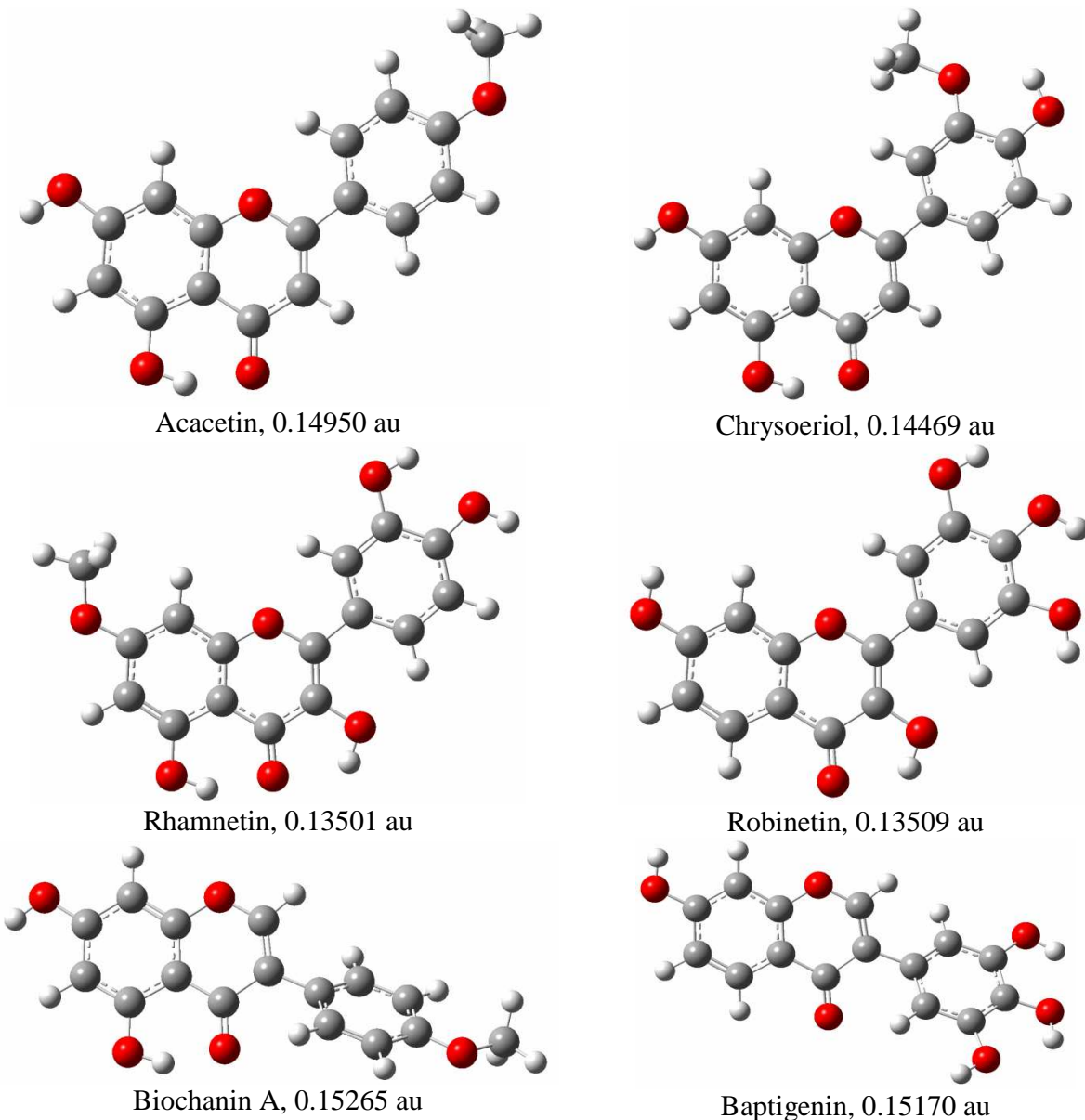


Figure S6. Geometries of the investigated flavonoids optimized with the B3LYP functional, with the HOMO-LUMO gap values ($E_h/\text{particle}$) indicated.

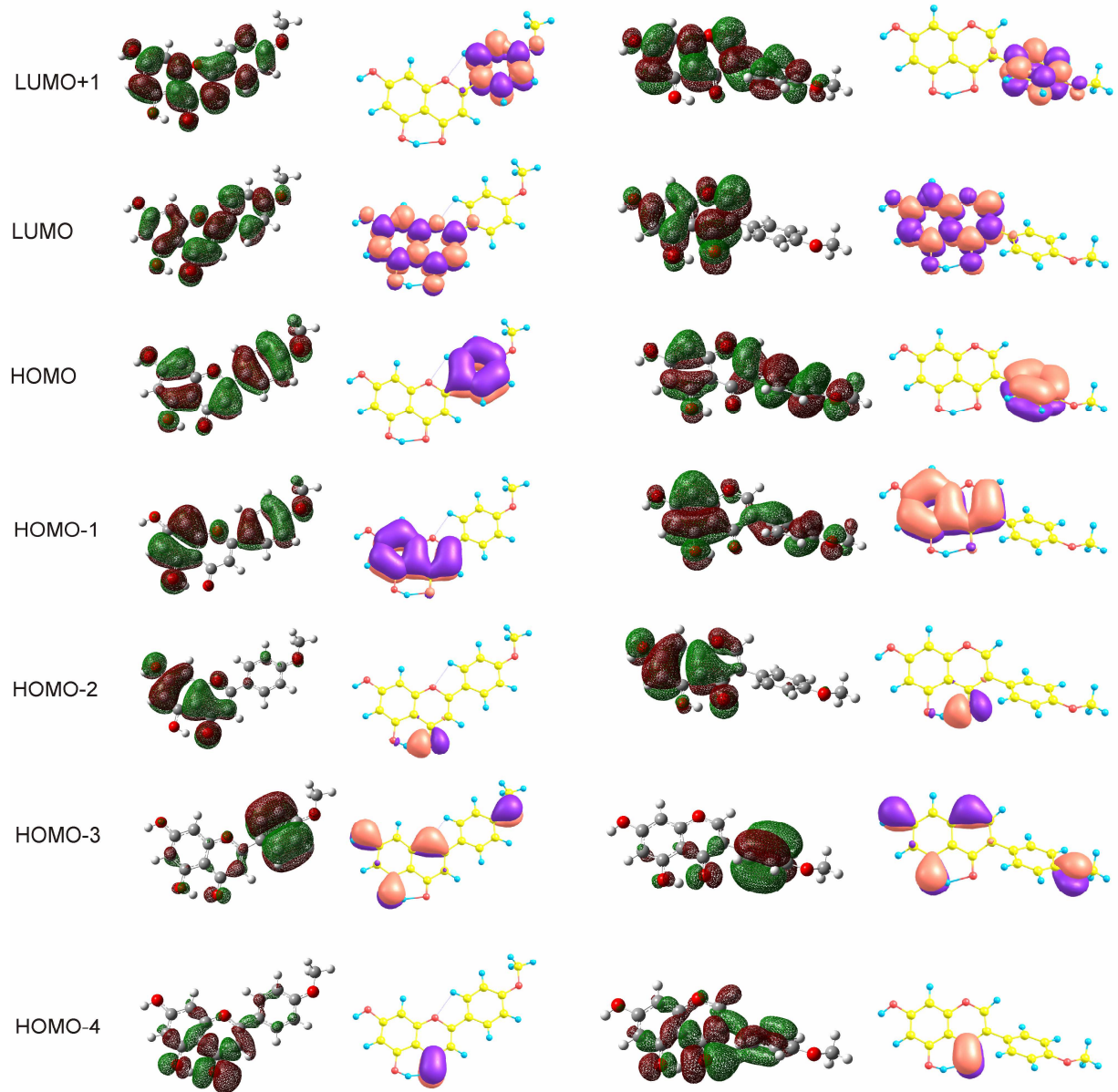


Figure S7. Kohn-Sham orbitals and NLMO clusters for acacetin (left) and biochanin A (right).

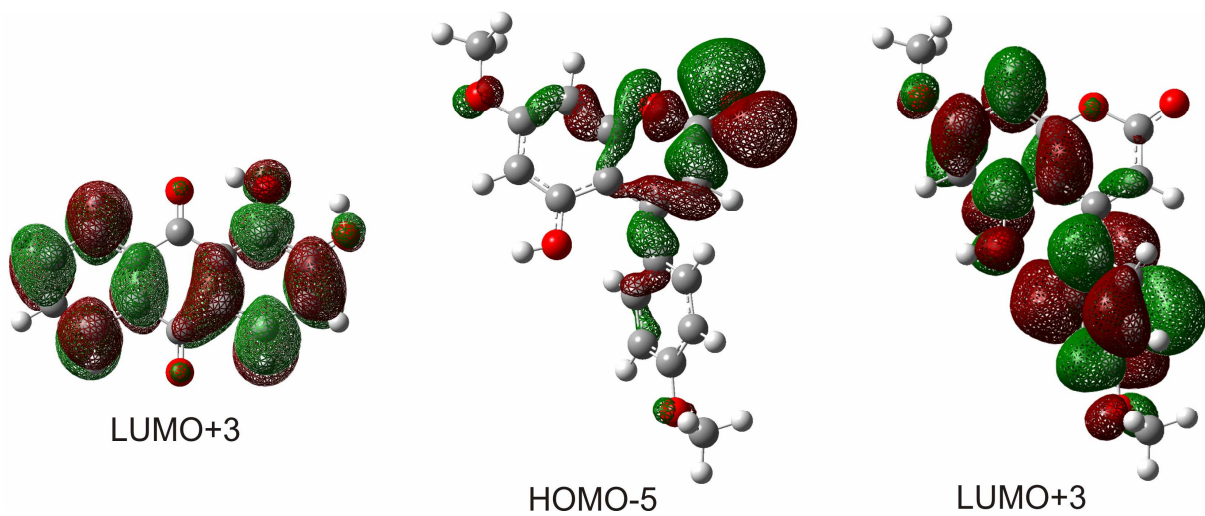


Figure S8. Some molecular orbitals of alizarin and 5'-OH-7,4'-diOMe-4-phenylcoumarin.

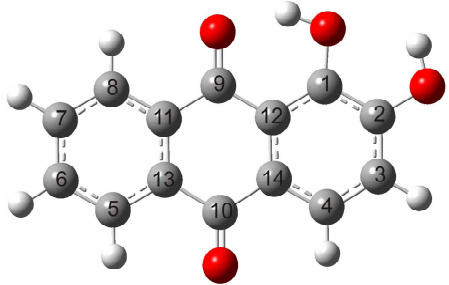


Table S1. Details on the selected NLMOs of alizarin obtained from the B3LYP density matrix

NLMO	Energy (E _h /particle)	Mean energy (E _h /particle)	Hybrid composition and occupancy of the parent NBO	NLMO cluster	
70. π^* C5-C6	0.01305		0.70(p) _{C6} -0.71(p) _{C5}	0.281	
69. π^* C7-C8	0.01273	0.01087	0.71(p) _{C8} -0.70(p) _{C7}	0.279	LUMO+2
68. π^* C11-C13	0.00682		0.71(p) _{C13} -0.70(p) _{C11}	0.426	
67. π^* C4-C14	0.01357		0.68(p) _{C14} -0.73(p) _{C4}	0.351	
66. π^* C2-C3	0.00239	0.00391	0.70(p) _{C3} -0.72(p) _{C2}	0.347	LUMO+1
65. π^* C1-C12	-0.00422		0.74(p) _{C1} -0.67(p) _{C12}	0.415	
64. π^* C10-O10	-0.00413		0.83(p) _{C10} -0.55(p) _{O10}	0.206	
63. π^* C9-O9	-0.02405	-0.01409	0.84(p) _{C9} -0.54(p) _{O9}	0.258	LUMO
62. π C5-C6	-0.27012		0.71(p) _{C6} +0.70(p) _{C5}	1.616	
61. π C7-C8	-0.27091	-0.27217	0.70(p) _{C8} +0.71(p) _{C7}	1.622	HOMO
60. π C11-C13	-0.27548		0.70(p) _{C13} +0.71(p) _{C11}	1.613	
59. π C4-C14	-0.27298		0.73(p) _{C14} +0.68(p) _{C4}	1.658	
58. π C2-C3	-0.28459	-0.28156	0.72(p) _{C3} +0.70(p) _{C2}	1.636	HOMO-1
57. π C1-C12	-0.28711		0.67(p) _{C1} +0.74(p) _{C12}	1.636	
56. LP O10	-0.28662		p	1.897	
55. LP O9	-0.33628	-0.31145	p	1.876	HOMO-2
54. LP O1	-0.34428		p	1.831	
53. LP O2	-0.34614	-0.34521	p	1.854	HOMO-3
52. π C10-O10	-0.38964		0.55(p) _{C10} +0.83(p) _{O10}	1.953	
51. π C9-O9	-0.40509	-0.39737	0.54(p) _{C9} +0.84(p) _{O9}	1.965	HOMO-4

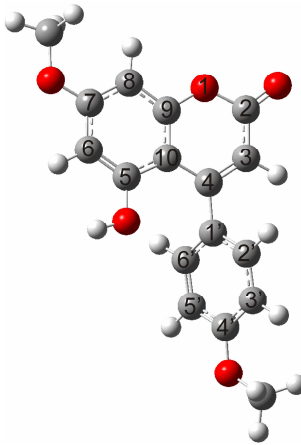


Table S2. Details on the selected NLMOs of 5'-OH-7,4'-diOMe-4-phenylcoumarin obtained from the B3LYP density matrix

NLMO	Energy (E _h /particle)	Mean energy (E _h /particle)	Hybrid composition and occupancy of the parent NBO	NLMO cluster
86. π^* C1'-C2'	0.02728	0.02288	0.69(p) _{C1'} -0.73(p) _{C2'}	LUMO+2
85. π^* C5'-C6'	0.02721		0.72(p) _{C6'} -0.69(p) _{C5'}	
84. π^* C3-C4	0.02081		0.75(p) _{C4} -0.66(p) _{C3}	
83. π^* C3'-C4'	0.01621		0.67(p) _{C3'} -0.73(p) _{C4'}	
82. π^* C5-C6	0.00862		0.76(p) _{C6} -0.66(p) _{C5}	0.351
81. π^* C7-C8	0.00623	0.00434	0.65(p) _{C8} -0.76(p) _{C7}	0.401 LUMO+1
80. π^* C9-C10	-0.00184		0.65(p) _{C10} -0.76(p) _{C9}	0.458
79. π^* C2-O2	-0.00949	-0.00949	0.85(p) _{C2} -0.53(p) _{O2}	0.339 LUMO
78. π C1'-C2'	-0.25882		0.73(p) _{C1'} +0.69(p) _{C2'}	1.678
77. π C5'-C6'	-0.26135	-0.26270	0.72(p) _{C5'} +0.69(p) _{C6'}	1.709 HOMO
76. π C3'-C4'	-0.26792		0.73(p) _{C3'} +0.68(p) _{C4'}	1.658
75. LP O2	-0.27610	-0.27610	p	1.850 HOMO-1
74. π C7-C8	-0.27734		0.65(p) _{C7} +0.76(p) _{C8}	1.671
73. π C9-C10	-0.27782	-0.28001	0.65(p) _{C9} +0.76(p) _{C10}	HOMO-2
72. π C5-C6	-0.28102		0.66(p) _{C5} +0.76(p) _{C6}	
71. π C3-C4	-0.28386		0.75(p) _{C3} +0.66(p) _{C4}	
70. LP 4'	-0.32444		p	1.842
69. LP O7	-0.33300	-0.33847	p	HOMO-3
68. LP O5	-0.34166		p	
67. LP O1	-0.35477		p	
66. π C2-O2	-0.39267	-0.39267	0.53(p) _{C2} +0.85(p) _{O2}	1.983 HOMO-4

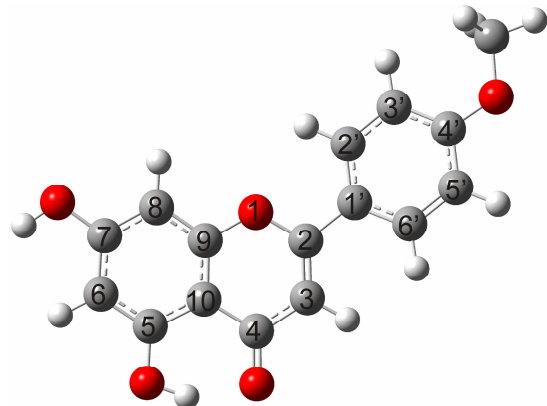


Table S3. Details on the selected NLMOs of acacetin obtained from the B3LYP density matrix

NLMO	Energy (E _h /particle)	Mean energy (E _h /particle)	Hybrid composition and occupancy of the parent NBO	NLMO cluster	
82. π^* C5'-C6'	0.01851		0.72(p) _{C6'} -0.69(p) _{C5'}	0.282	
81. π^* C1'-C2'	0.01404	0.01382	0.70(p) _{C1'} -0.72(p) _{C2'}	0.393	LUMO+1
80. π^* C3'-C4'	0.00891		0.67(p) _{C3'} -0.74(p) _{C4'}	0.383	
79. π^* C2-C3	0.00842		0.75(p) _{C2} -0.66(p) _{C3}	0.244	
78. π^* C5-C6	0.00598		0.76(p) _{C5} -0.65(p) _{C6}	0.366	
77. π^* C7-C8	0.00280	-0.00019	0.65(p) _{C8} -0.76(p) _{C7}	0.407	LUMO
76. π^* C9-C10	-0.00251		0.76(p) _{C9} -0.65(p) _{C10}	0.474	
75. π^* C4-O4	-0.01564		0.86(p) _{C4} -0.51(p) _{O4}	0.387	
74. π C1'-C2'	-0.26513		0.74(p) _{C1'} +0.67(p) _{C2'}	1.644	
73. π C5'-C6'	-0.27070	-0.26963	0.72(p) _{C5'} +0.69(p) _{C6'}	1.716	HOMO
72. π C3'-C4'	-0.27307		0.74(p) _{C3'} +0.67(p) _{C4'}	1.628	
71. π C7-C8	-0.27409		0.65(p) _{C7} +0.76(p) _{C8}	1.651	
70. π C5-C6	-0.27659		0.65(p) _{C5} +0.76(p) _{C6}	1.684	
69. π C9-C10	-0.28173		0.65(p) _{C9} +0.76(p) _{C10}	1.636	
68. π C2-C3	-0.29614		0.66(p) _{C2} +0.75(p) _{C3}	1.782	
67. LP O4	-0.31638	-0.31638	p	1.873	HOMO-2
66. LP O5	-0.32786		p	1.829	
65. LP O4'	-0.33052		p	1.828	
64. LP O1	-0.36464		p	1.747	
63. LP O7	-0.34393		p	1.860	
62. π C4-O4	-0.37870	-0.37870	0.51(p) _{C4} +0.86(p) _{O4}	1.975	HOMO-4

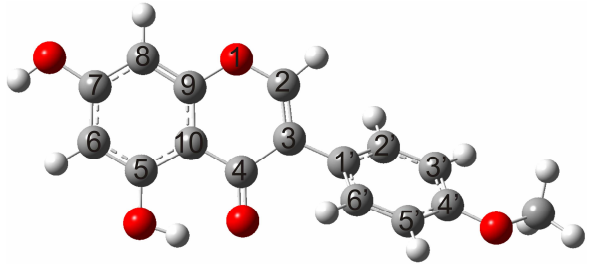


Table S4. Details on the selected NLMOs of biochanin A obtained from the B3LYP density matrix

NLMO	Energy (E _h /particle)	Mean energy (E _h /particle)	Hybrid composition and occupancy of the parent NBO	NLMO cluster	
82. π^* C5'-C6'	0.02667		0.72(p) _{C6'} -0.69(p) _{C5'}	0.303	
81. π^* C1'-C2'	0.02605	0.02313	0.69(p) _{C1'} -0.73(p) _{C2'}	0.367	LUMO+1
80. π^* C3'-C4'	0.01666		0.68(p) _{C3'} -0.73(p) _{C4'}	0.386	
79. π^* C2-C3	0.00923		0.74(p) _{C2} -0.67(p) _{C3}	0.192	
78. π^* C5-C6	0.00491		0.76(p) _{C5} -0.65(p) _{C6}	0.360	
77. π^* C7-C8	0.00190	-0.00132	0.65(p) _{C8} -0.76(p) _{C7}	0.404	LUMO
76. π^* C9-C10	-0.00587		0.76(p) _{C9} -0.65(p) _{C10}	0.480	
75. π^* C4-O4	-0.01678		0.85(p) _{C4} -0.52(p) _{O4}	0.359	
74. π C1'-C2'	-0.25818		0.73(p) _{C1'} +0.69(p) _{C2'}	1.678	
73. π C5'-C6'	-0.26074	-0.26211	0.72(p) _{C5'} +0.69(p) _{C6'}	1.709	HOMO
72. π C3'-C4'	-0.26741		0.73(p) _{C3'} +0.68(p) _{C4'}	1.657	
71. π C7-C8	-0.27540		0.65(p) _{C7} +0.76(p) _{C8}	1.649	
70. π C5-C6	-0.27831		0.65(p) _{C5} +0.76(p) _{C6}	1.687	HOMO-1
69. π C9-C10	-0.28363	-0.28460	0.65(p) _{C9} +0.76(p) _{C10}	1.633	
68. π C2-C3	-0.30106		0.67(p) _{C2} +0.74(p) _{C3}	1.810	
67. LP O4	-0.31668	-0.31668	p	1.868	HOMO-2
66. LP O4'	-0.32382		p	1.843	
65. LP O5	-0.32932	-0.34133	p	1.826	HOMO-3
64. LP O7	-0.34491		p	1.858	
63. LP O1	-0.36726		p	1.732	
62. π C4-O4	-0.38573	-0.38573	0.52(p) _{C4} +0.85(p) _{O4}	1.976	HOMO-4

Table S5. Results of the TDDFT calculations with the B3LYP method for alizarin: vertical transition wavelength (λ_{\max}), oscillator strength (f), and detailed orbital description. All calculated absorption bands are presented. Experimental λ_{\max} values are given for comparison

B3LYP			Experimental
λ_{\max} (nm)	f	Orbital description	λ_{\max} (nm)
439	0.14	HOMO → LUMO (70%)	432
294	0.19	HOMO-4 → LUMO (68%)	277
257	0.41	HOMO-1 → LUMO+1 (61%) HOMO → LUMO+2 (30%)	264
		HOMO-3 → LUMO+2 (11%)	
245	0.38	HOMO-1 → LUMO+3 (12%) HOMO → LUMO+2 (55%)	248

Table S6. Results of the TDDFT calculations with the B3LYP method for 5'-OH-7,4'-diOMe-4-phenylcoumarin: vertical transition wavelength (λ_{\max}), oscillator strength (f), and detailed orbital description. All calculated absorption bands are presented. Experimental λ_{\max} values are given for comparison

B3LYP			Experimental
λ_{\max} (nm)	f	Orbital description	λ_{\max} (nm)
		HOMO-2 → LUMO (32%)	
328	0.23	HOMO-1 → LUMO (53%) HOMO → LUMO (33%)	326
256	0.119	HOMO-5 → LUMO (14%) HOMO → LUMO+1 (64%)	261
		HOMO-4 → LUMO (47%)	
228	0.15	HOMO-1 → LUMO+1 (11%) HOMO → LUMO+3 (15%)	223

Table S7. Results of the TDDFT calculations with the B3LYP method for acacetin: vertical transition wavelength (λ_{\max}), oscillator strength (f), and detailed orbital description. All calculated absorption bands are presented. Experimental λ_{\max} values are given for comparison

B3LYP			Experimental
λ_{\max} (nm)	f	Orbital description	λ_{\max} (nm)
322	0.36	HOMO → LUMO (21%) HOMO-1 → LUMO (66%)	327
		HOMO-3 → LUMO (21%)	
265	0.12	HOMO-2 → LUMO+1 (10%) HOMO → LUMO+1 (53%)	269

Table S8. Results of the TDDFT calculations with the B3LYP method for biochanin A: vertical transition wavelength (λ_{\max}), oscillator strength (f), and detailed orbital description. All calculated absorption bands are presented. Experimental λ_{\max} values are given for comparison

B3LYP			Experimental
λ_{\max} (nm)	f	Orbital description	λ_{\max} (nm)
345	0.04	HOMO → LUMO (70%)	330 (shoulder)
271	0.81	HOMO-2 → LUMO (21%) HOMO → LUMO+1 (66%)	261